Supporting information: First principles study on hydrogen doping induced metal-to-insulator transition in rare earth nickelates $RNiO_3$ (R = Pr, Nd, Sm, Eu, Gd, Tb, Dy, Yb)

Pilsun Yoo and Peilin Liao*

School of Materials Engineering, Purdue University, West Lafayette, IN 47906, United States

*E-mail of corresponding author: *lpl@purdue.edu*

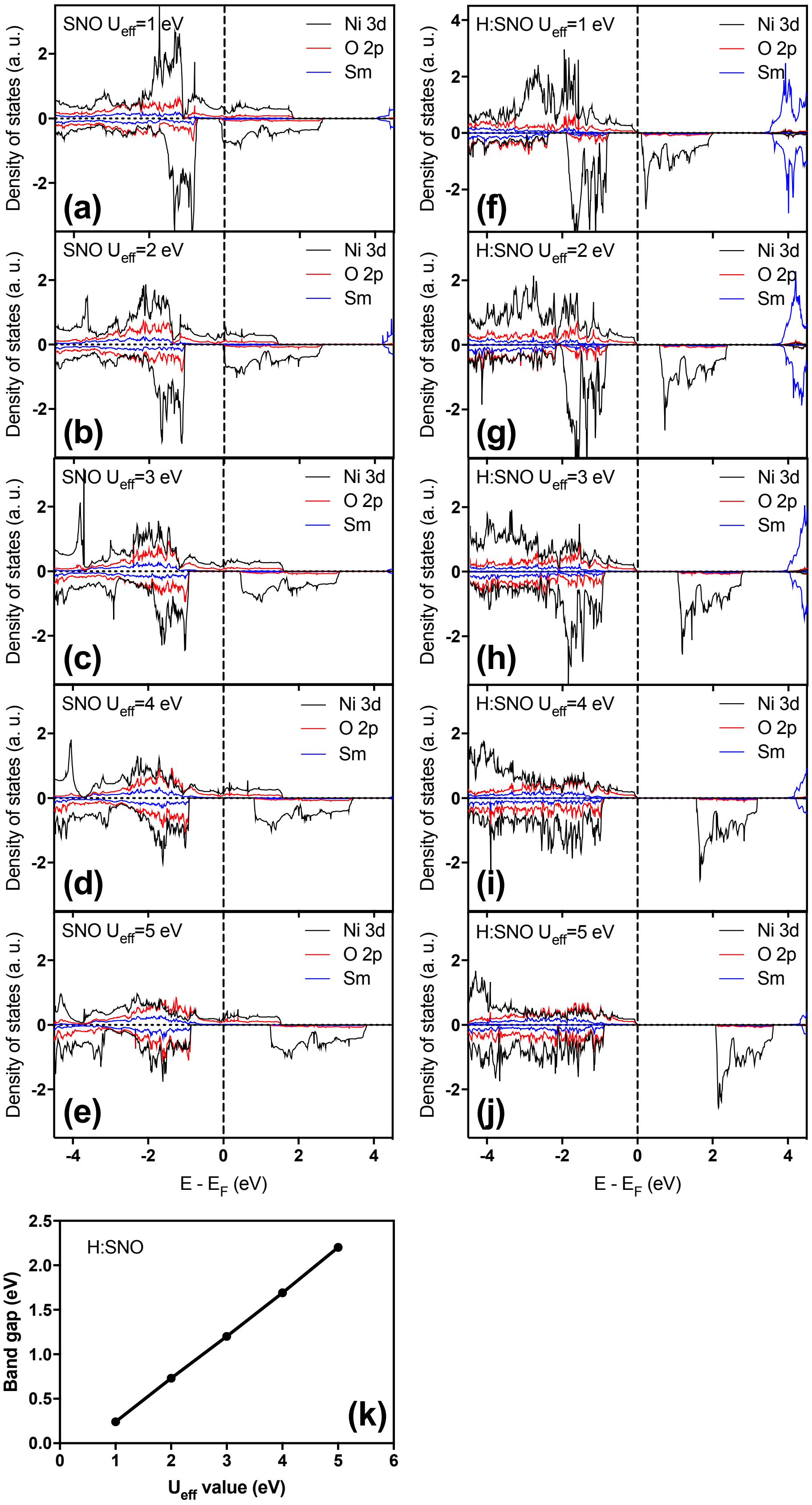

Figure S1. Projected density of states for pure $SmNiO_3$ (a)-(e) and H:$SmNiO_3$ (f)-(j) using the different U_{eff} values (1~5 eV). The predicted band gap values vs U_{eff} values for H:$SmNiO_3$ (k).

Table S1. Crystal structures of $SmNiO_3$ and their percentage error from the experimental structure of $SmNiO_3$ (*Phys. Rev B.*, 1998, **57**, R3189-R3192) with different U_{eff} values applied.

U_{eff} value	***a*** (Å)	***b*** (Å)	***c*** (Å)	Volume (Å^3)	***a*** error (%)	***b*** error (%)	***c*** error (%)	Volume error (%)
1 eV	5.270	5.381	7.459	211.52	-1.16	-0.79	-1.28	-3.21
2 eV	5.238	5.417	7.483	212.32	-1.76	-0.13	-0.97	-2.84
3 eV	5.268	5.369	7.481	211.59	-1.20	-1.01	-0.99	-3.17
4 eV	5.270	5.356	7.482	211.19	-1.16	-1.25	-0.98	-3.36
5 eV	5.271	5.349	7.484	211.01	-1.14	-1.38	-0.95	-3.44

Table S2. Crystal structures of H:$SmNiO_3$ with different U_{eff} values applied.

U_{eff} value	***a*** (Å)	***b*** (Å)	***c*** (Å)	Volume (Å^3)
1 eV	5.169	6.063	7.584	237.68
2 eV	5.290	5.979	7.537	238.39
3 eV	5.240	6.011	7.553	237.90
4 eV	5.257	5.992	7.547	237.73
5 eV	5.258	5.980	7.549	237.36

Table S3. Energy differences between various AFM states in the monoclinic lattice ($P2_1/n$) and the FM state in the orthorhombic lattice (Pbnm) for three different $RNiO_3$. The ground states are marked with bold texts. These oxide are in the insulating phase in their ground states.

	T-AFM (E_{AFM}-E_{FM})	E-AFM (E_{AFM}-E_{FM})	A-AFM (E_{AFM}-E_{FM})	S-AFM (E_{AFM}-E_{FM})
$PrNiO_3$	**-0.46 eV**	-0.34 eV	0.17 eV	-0.45 eV
$SmNiO_3$	**-0.21 eV**	-0.12 eV	0.16 eV	-0.20 eV
$DyNiO_3$	0.83 eV	-0.05 eV	0.14 eV	**-0.07 eV**

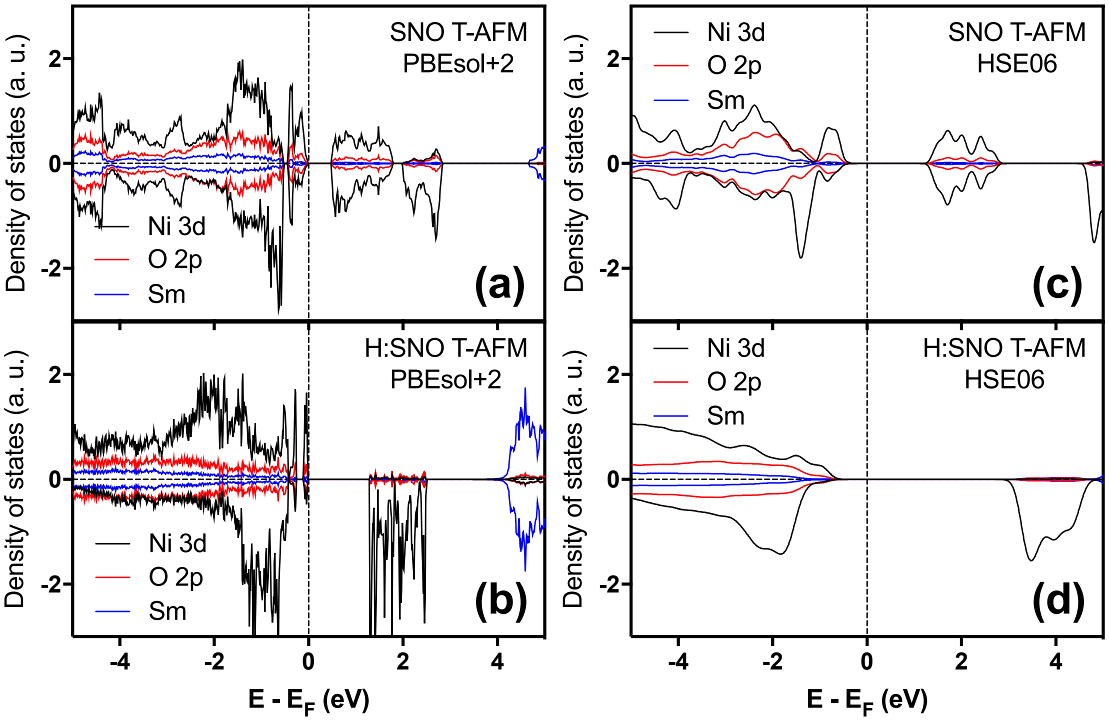

Figure S2. Projected density of states for pristine and H doped $SmNiO_3$ in T-AFM states for PBEsol+2 (a) and (b), and for HSE06 (c) and (d). The band gap values were predicted to increase upon H doping by both PBEsol+2 (from 0.48 eV to 1.30 eV) and HSE06 (from 1.37 eV to 2.96 eV) along with changes in the electron occupation of Ni 3d orbitals.

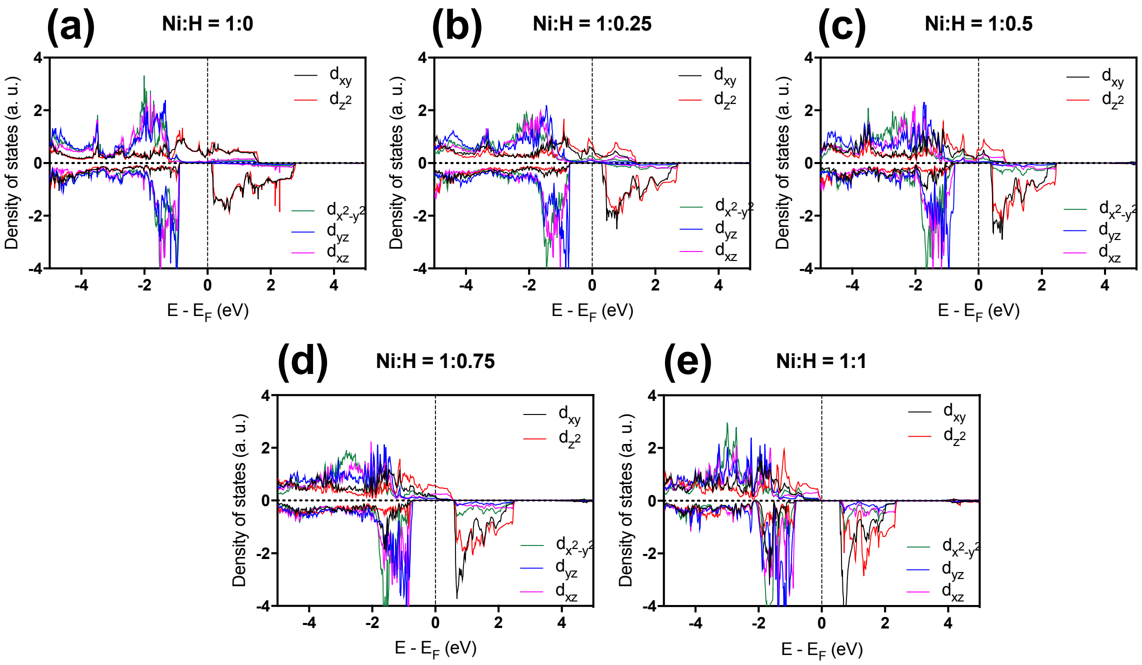

Figure S3. Projected Ni d-orbitals (d_{xy}, d_{z^2}, $d_{x^2-y^2}$, d_{yz} and d_{xz}) density of states of $SmNiO_3$ at different H doping concentrations. Due to the $\sqrt{2} \times \sqrt{2} \times 2$ supercell of standard perovskite used in the calculations, the d_{xy} and d_{z^2} correspond to conventional e_g orbitals, while $d_{x^2-y^2}$, d_{yz} and d_{xz} correspond to conventional t_{2g} orbitals. As the H doping concentration increases, the spin up e_g states shift from unoccupied states to the valance bands.

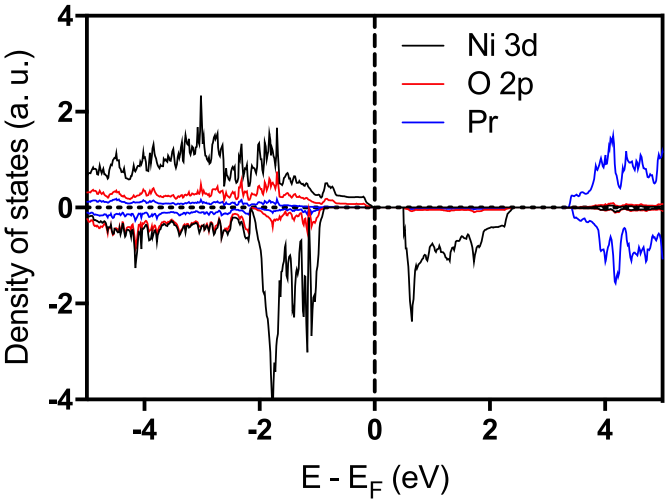

Figure S4. Projected density of states for hydrogen doped $PrNiO_3$ at the level of PBEsol+3.

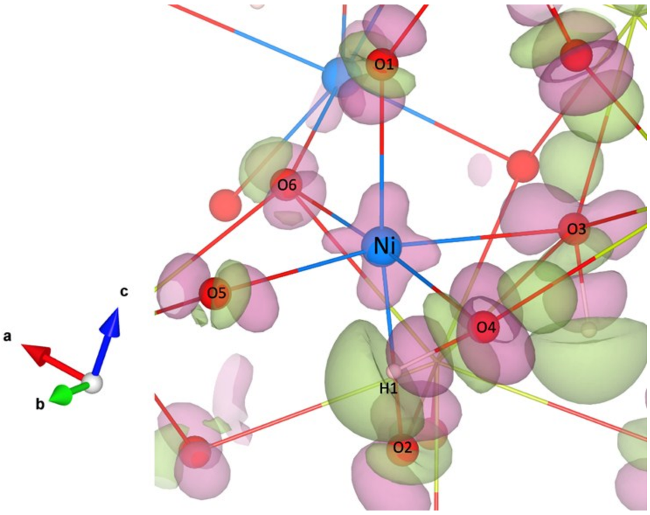

Figure S5. Electron density difference plot obtained by subtracting the electron density of pure $SmNiO_3$ and the electron density of single H atom from the electron density of H doped $SmNiO_3$. The purple contour has positive sign, indicating gaining electrons upon H doping, while the light blue contour has negative sign, indicating losing electrons with hydrogen doping on $SmNiO_3$. The O1 and O2 are located at top and bottom apex of NiO_6 octahedron, and O3 to O6 are oxygens in the middle plane of the octahedron. The charge difference shows that Ni is gaining electrons in the form of d_{z^2} orbital from hydrogen atom H1, which is bonded to O4.

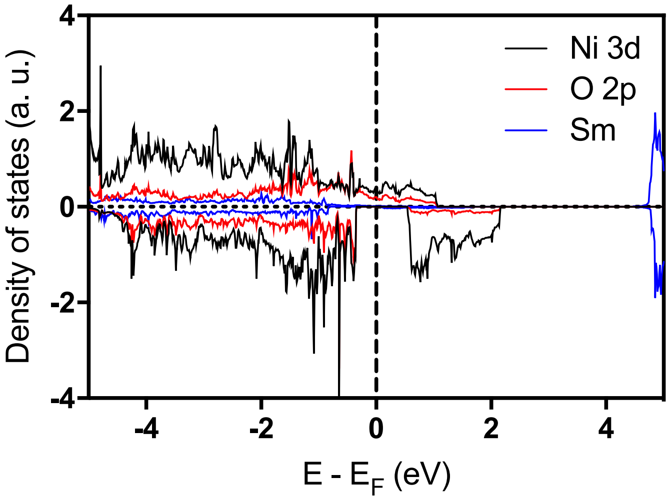

Figure S6. Projected density of states at the PBEsol+2 level for the distorted H:$SmNiO_3$ structure obtained by removing all hydrogens from H:$SmNiO_3$. The metallic character was retained with the distortion, suggesting that the distortion alone cannot cause the metal-to-insulator transition.

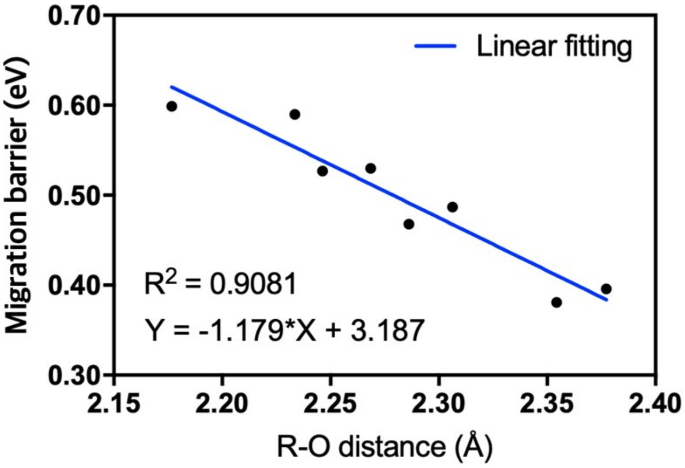

Figure S7. Migration barrier of Route 1 vs R-O distance.